Nonsymmetric wormholes and localized big rip singularities in Einstein-Weyl gravity

A. Bonanno,[1,2] S. Silveravalle,[3,4] and A. Zuccotti[5]

[1]*INAF, Osservatorio Astrofisico di Catania, via S.Sofia 78, I-9 5123 Catania, Italy*
[2]*INFN, Sezione di Catania, via S. Sofia 64, I-95123 Catania, Italy*
[3]*Università degli Studi di Trento, Via Sommarive, 14, IT-38123 Trento, Italy*
[4]*INFN—TIFPA, Via Sommarive, 14, IT-38123 Trento, Italy*
[5]*Università di Pisa, Largo Bruno Pontecorvo, 3, IT-56127 Pisa, Italy*

(Received 22 April 2022; accepted 1 June 2022; published 24 June 2022)

The inclusion of the Weyl squared term in the gravitational action is one of the most simple, yet nontrivial modifications to general relativity at high energies. Nevertheless the study of the spherically symmetric vacuum solutions of this theory has received much attention only in recent times. A new type of asymptotically flat wormhole which does not match symmetrically at a finite radius with another sheet of the spacetime is presented. The outer spacetime is characterized by a Newtonian potential with a Yukawa correction, and has gravitational properties that can be arbitrarily close to the ones of a Schwarzschild black hole. The internal spacetime instead possesses a singularity at $r = \infty$ with the topology of a 2-dimensional sphere. The expansion scalar of geodesics reaching this singularity diverges in a finite amount of proper time, with a striking resemblance with the future singularity of the big rip cosmological scenario. In terms of the external Yukawa hair and mass M, these new wormholes fill a large region of the two-dimensional parameter space of physical solutions with $M > 0$. On the contrary black holes, both of Schwarzschild and non-Schwarzschild nature, are confined on a line. We argue that this type of wormholes are ideal black hole mimickers.

DOI: 10.1103/PhysRevD.105.124059

I. INTRODUCTION

The recent discovery of a new class of black holes [1] has shown that the spectrum of classical solutions derived from quadratic corrections to the classical Einstein-Hilbert Lagrangian is far from being clearly understood. The case of Einstein-Weyl theory, defined by

$$S = \int d^4x\sqrt{-g}[\gamma R - \alpha C_{\mu\nu\rho\sigma}C^{\mu\nu\rho\sigma}] \tag{1}$$

is particularly instructive. Spherically symmetric, asymptotically flat solutions with vanishing Ricci scalar R and non-zero Ricci tensor $R_{\mu\nu}$ posses regular horizons and obey the first law of thermodynamics [1]. However, in spite of much analytical [2–4] and numerical [5,6] efforts the role played by the asymptotic field in determining the global property of the solutions and the structure of the singularity still deserves further investigation [7].

This scenario has to be contrasted with the more familiar one in $f(R)$ theories, as in this case spherically symmetric solutions have been extensively studied in the past [8,9], along with their stability properties in various astrophysical contexts [10,11].

The inclusion of the squared Weyl tensor term to the standard Einstein-Hilbert Lagrangian has a long history. Albeit originally motivated by the possibility of perturbative renormalization [12], in more recent times its presence has emerged [13–15] in the framework of the asymptotically safe program for quantum gravity [16,17] and of the fakeons theory [18,19]. In this work we shall not discuss the viability of the theory defined in (1) at the quantum level because we would like to focus on the classical content of the theory extending the investigation started in [7] to include wormhole solutions. In fact, although a wormhole class of solutions have been found in [5], their weight in the space of all the possible spherically symmetric and asymptotically flat solutions, and their global properties are still unknown. Indeed the so called "nonsymmetric" wormholes (no-sy WHs) found in [5] cannot be analytically described in simple terms and their interpretation is still elusive. In this work we shall fill this gap and study this class of solutions in detail.

The numerical approach described in [7] for black holes is clearly advantageous also in the case of wormholes, allowing to investigate the dependence of the local metric coefficient on the asymptotic field, which is described by the sum of a Schwarzschild and Yukawa term, in a systematic manner. In particular, it is possible to determine the properties of the metric close to the wormhole throat as a function of the mass and the Yukawa coefficient at large

 © 2022 American Physical Society

distances. Once the metric functions and their derivatives have been determined at the throat radius, it is possible to extend the integration to the other patch of spacetime and characterize its behavior at large distances. We show that these wormholes connect an asymptotically flat metric with a singular spacetime where the temporal and radial components of the metric vanish exponentially at infinity. This new type of singularity is perceived by infalling observers in a similar way as the future singularity of the big rip cosmological scenario [20], with the expansion scalar of congruences of geodesics going to an infinite positive value in a finite amount of proper time. For external observers, instead, the singularity lies at the edges of the causal structure, and therefore is naked only in the infinite past limit. Having no trapped surfaces, however, these singularities are always avoidable with a sufficient amount of energy. It is interesting to note that a similar spacetime has been found in [21] as solution of general relativity coupled with a quantum corrected stress-energy tensor, and an analytical no-sy WH spacetime have been found in the pure squared Weyl tensor theory [22], suggesting that no-sy WHs are indeed a common prediction of semiclassical theories of gravity.

At last, as the parameter space of possible solutions is getting understood [23], we also show that no-sy WHs densely populate this two-dimensional space, at variance with the BH class that is confined on two lines. In addition, no-sy WHs populate a large portion of the part of the parameter space with physical solutions with a positive mass, and are present for arbitrarily large masses. Schwarzschild black holes appear therefore only as a limiting case of no-sy WHs in this large mass limit.

II. EQUATIONS OF MOTION AND ANALYTICAL APPROXIMATIONS

A. Nonlinear equations of motion

The equations of motion of the Einstein-Weyl theory can be derived from the minimization of the action (1). In tensorial form they are written as

$$\mathcal{H}_{\mu\nu} = \gamma\left(R_{\mu\nu} - \frac{1}{2}Rg_{\mu\nu}\right) - 4\alpha\left(\nabla^\rho\nabla^\sigma + \frac{1}{2}R^{\rho\sigma}\right)C_{\mu\rho\nu\sigma} = 0, \tag{2}$$

and, thanks to the traceless nature of the Weyl tensor, their trace is simply

$$\mathcal{H}^\mu{}_\mu \propto R = 0. \tag{3}$$

We now focus on static and spherically symmetric spacetimes, and choose the ansatz for the metric in Schwarzschild coordinates

$$ds^2 = -h(r)dt^2 + \frac{dr^2}{f(r)} + r^2 d\Omega^2. \tag{4}$$

Exploiting the trace equation (3) we can recast the equations of motion (2) as a system of two second order ordinary differential equations in $h(r)$ and $f(r)$, as already shown in [5,7]. Explicitly these equations are

$$\begin{aligned}
&4h(r)^2(rf'(r) + f(r) - 1) - r^2 f(r)h'(r)^2 \\
&\quad + rh(r)(rf'(r)h'(r) + 2f(r)(rh''(r) + 2h'(r))) = 0, \\
&\alpha r^2 f(r)h(r)(rf'(r) + 3f(r))h'(r)^2 \\
&\quad + 2r^2 f(r)h(r)^2 h'(r)(\alpha r f''(r) + \alpha f'(r) - \gamma r) \\
&\quad + h(r)^3(r(3\alpha r f'(r)^2 - 4\alpha f'(r) + 2\gamma r) \\
&\quad - 2f(r)(4\alpha + 2\alpha r^2 f''(r) - 2\alpha r f'(r) + \gamma r^2) \\
&\quad + 8\alpha f(r)^2) - \alpha r^3 f(r)^2 h'(r)^3 = 0.
\end{aligned} \tag{5}$$

Even if the symmetries of the spacetime greatly simplify the equations, it is clear that the full nonlinear system cannot be solved exactly, and either approximations or numerical methods have to be used. In this section we will show the analytical approximations needed to study numerically the full system of equations (5), and to extract their physical properties.

B. Linearized equations and solutions in the weak field limit

In this work we are interested in asymptotically flat spacetimes, i.e., solutions that describe isolated objects without a cosmological constant. We can therefore consider the weak field limit at large distances, in which the metric is a perturbation of the Minkowski spacetime. As described in [5,7,24] we write the functions $h(r)$ and $f(r)$ as

$$h(r) = 1 + \epsilon V(r), \qquad f(r) = 1 + \epsilon W(r), \tag{6}$$

and expand (2) at linear order in ϵ. It is convenient to consider the combinations

$$\begin{aligned}
\mathcal{H}^\mu{}_\mu &\propto \nabla^2 V(r) + 2Y(r) = 0, \\
\mathcal{H}^i{}_i - \mathcal{H}^t{}_t &\propto \left(\nabla^2 - \frac{3\gamma}{4\alpha}\right)\nabla^2 V(r) - \nabla^2 Y(r) = 0,
\end{aligned} \tag{7}$$

where $Y(r) = r^{-2}(rW(r))'$, which can be easily solved using Fourier modes. Imposing asymptotic flatness and fixing a parametrization of time (i.e., imposing $h(r) \to 1$ as $r \to +\infty$) we can suppress some of the free parameters of the solution of (7) and obtain

$$h(r) = 1 - \frac{2M}{r} + 2S_2^- \frac{e^{-m_2 r}}{r},$$
$$f(r) = 1 - \frac{2M}{r} + S_2^- \frac{e^{-m_2 r}}{r}(1 + m_2 r), \tag{8}$$

with $m_2^2 = \frac{\gamma}{2\alpha}$ and M being the ADM mass in Planck units, which is the Schwarzschild solution with exponentially suppressed corrections. We note that in the Newtonian limit the gravitational potential $\phi(r) \sim \frac{1}{2}(h(r) - 1)$ will have a Yukawa correction, as expected for a massive mediator of the interaction, which can be either attractive or repulsive according to the sign of the "charge" S_2^-. We will see in Sec. III B that the sign and the relative values of M and S_2^- will be crucial for having a no-sy WH type of solution.

C. Series expansion at finite radii

At finite radii we can expect the solutions to be well approximated by series expansions. The different families of solutions allowed by the equations of motion have been exhaustively studied and classified in [3,5] using a variation of the Frobenius method. Taking an expansion of the metric functions in the form

$$h(r) = (r - r_0)^t \left[\sum_{n=0}^{N} h_{t+\frac{n}{\Delta}} (r - r_0)^{\frac{n}{\Delta}} + O((r - r_0)^{\frac{N+1}{\Delta}})\right],$$
$$f(r) = (r - r_0)^s \left[\sum_{n=0}^{N} f_{s+\frac{n}{\Delta}} (r - r_0)^{\frac{n}{\Delta}} + O((r - r_0)^{\frac{N+1}{\Delta}})\right], \tag{9}$$

it is possible to classify the solutions as $(s,t)^{\Delta}_{r_0}$. The families known at present time are shown in Table I, where in the second column we made manifest the number of free parameters after imposing asymptotic flatness and a specific time parameterization. We note that in [25] a non-Frobenius family with logarithmic corrections to the $(-1,-1)^1_0$, and with one additional free parameter, has been found and there are hints that it might populate a large area of the parameter space. We also specify that there are some differences in the notation used in our work and in [3,5], the main being the different sign for the exponent s due to their metric ansatz in terms of the function $A(r) = 1/f(r)$ for the families around $r_0 = 0$.

TABLE I. Families of solutions around finite and zero radii in Einstein-Weyl gravity.

Family	No of free parameters	Interpretation
$(0,0)^1_0$	$2(\to 0)$	Regular solution/True vacuum
$(-1,-1)^1_0$	$3(\to 1)$	Naked singularity/Schwarzschild interior
$(-2,2)^1_0$	$4(\to 2)$	Bachian singularity/Holdom star
$(0,0)^1_{r_0}$	$4(\to 2)$	Regular metric
$(1,1)^1_{r_0}$	$3(\to 1)$	Black hole
$(1,0)^1_{r_0}$	$2(\to 0)$	Symmetric wormhole
$(1,0)^2_{r_0}$	$4(\to 2)$	Nonsymmetric wormhole
$(4/3,0)^3_{r_0}$	$3(\to 1)$	Not known

As specified in the introduction, our main goal is to describe the physical properties of the nonsymmetric wormhole type of solutions, that is solutions belonging to the $(1,0)^2_{r_0}$ family; having the maximum number of free parameters allowed in the theory, this family is expected to populate a nonzero measure region of the parameter space. We highlight here the behavior of the metric around the "throat" $r = r_T$

$$h(r) = h_0 + h_{1/2}(r - r_T)^{\frac{1}{2}} + h_1(r - r_T) + O((r - r_T)^{\frac{3}{2}})$$
$$f(r) = f_1(r - r_T) + f_{3/2}(r - r_T)^{\frac{3}{2}} + O((r - r_T)^2), \tag{10}$$

which is characterized by a divergent radial component of the metric $g_{rr} = 1/f(r)$ and a regular, but with divergent derivative, temporal component of the metric $g_{tt} = -h(r)$. Moreover, this family of solution is completely determined by the four parameters $(r_T, h_0, h_{1/2}, f_1)$, of which only specific combinations will lead to asymptotically flat solutions.

1. Wormhole behavior of $(1,0)^2_{r_0}$ solutions

The metric in (10) is defined only for radii $r > r_T$, but having regular curvature invariants at $r = r_T$ we expect this to be a coordinates artefact. The simple extension to the region $r < r_T$ with an expansion in terms of semi-integer powers of $(r_T - r)$, suffers from a severe pathology, namely we have to choose between having discontinuities in the curvature invariants or having two temporal coordinates. The other possible extension is to consider a wormhole type of spacetime, where we join two $r > r_T$ patches at the "throat" $r = r_T$. We believe that this is the most sensible choice.

The wormhole nature of these type of solution is manifest after the coordinate transformation

$$r = r_T + \frac{1}{4}\rho^2, \tag{11}$$

in which the metric has the form

$$ds^2 = -h_0\left(1 + \frac{h_{1/2}}{2}\rho + O(\rho^2)\right)dt^2 + \frac{d\rho^2}{f_1 + \frac{f_{3/2}}{2}\rho + O(\rho^2)} + \left(r_T + \frac{1}{4}\rho^2\right)^2 d\Omega^2. \tag{12}$$

This is manifestly well behaved around $\rho = 0$, and then we can extend the metric to the $\rho < 0$ region, corresponding to a second $r > r_T$ patch of a wormhole-type spacetime [5]. In contrast with standard wormhole solutions, however, the metric (12) is not symmetric under the parity operation $\rho \to -\rho$. Going back to the r coordinate, we see that the metric on other side of the throat can be described switching the sign of the semi-integer terms in (10), that is

$$h(r) = h_0 - h_{1/2}(r-r_T)^{\frac{1}{2}} + h_1(r-r_T) - O((r-r_T)^{\frac{3}{2}}),$$
$$f(r) = f_1(r-r_T) - f_{3/2}(r-r_T)^{\frac{3}{2}} + O((r-r_T)^2). \quad (13)$$

Looking at the explicit form of the parameters it can be proved that the expansion (13) is exactly the one in (10) after the substitution $h_{1/2} \to -h_{1/2}$.

D. Solution around vanishing metric

Given the wormhole nature of the metric in (10), we present a spacetime characterized by two regions both mapped by $r \in [r_T, +\infty)$. It is natural to ask how the metric behaves in the second patch, and in particular if it can be asymptotically flat in both the spacetime patches.

From our numerical work we found a common behavior: once imposed asymptotic flatness in the first patch, the metric in the second patch results to be nonasymptotically flat, with $f(r)$ diverging and $h(r)$ vanishing for $r \to +\infty$, corresponding to both g_{rr} and g_{tt} vanishing at large radius. At the present time, nonasymptotically flat solutions are expected in Einstein-Weyl gravity, but there is no analytical approximation of such solutions.

Following what we have from the numerical results we proceed by looking for a metric with $g_{rr}(r)$ and $g_{tt}(r)$ vanishing for $r \to +\infty$. In order to do this we expand the metric functions as

$$h(r) = \epsilon h_1(r)(1 + \epsilon h_2(r) + O(\epsilon^2)),$$
$$f(r) = \frac{1}{\epsilon f_1(r)(1 + \epsilon f_2(r) + O(\epsilon^2))}, \quad (14)$$

then we can solve our equations of motion (5) order by order in ϵ, starting from $O(\epsilon^{-1})$. An exact solution of the equations at first order can be found, and it has the form

$$h_1(r) = C_h e^{-a r} r^2$$
$$f_1(r) = C_f e^{-a r} r^2 \quad (15)$$

in which a, C_h, C_f are free parameters, with the constraint $a > 0$, in order to be consistent with the initial assumption $g_{tt}, g_{rr} \to 0$ for $r \to +\infty$. Now it is convenient to rewrite the ansatz (14) as

$$h(r) = C_h e^{-a r} r^2 (1 + \tilde{h}_2(r) e^{-a r} + O(e^{-2a r}))$$
$$f(r) = \frac{1}{C_f e^{-a r} r^2 (1 + \tilde{f}_2(r) e^{-a r} + O(e^{-2a r}))}, \quad (16)$$

where the expansion in ϵ is substituted by an expansion in the variable $y = e^{-a r}$. When expanding (5) order by order in y, the first orders become a system of second order linear differential equations in $\tilde{h}_2(r)$ and $\tilde{f}_2(r)$. The solution can be found in a polynomial form

$$\tilde{h}_2(r) = \tilde{h}_0 + \tilde{h}_1 r + \tilde{h}_2 r^2 + \tilde{h}_3 r^3,$$
$$\tilde{f}_2(r) = \tilde{f}_0 + \tilde{f}_1 r + \tilde{f}_2 r^2 + \tilde{f}_3 r^3, \quad (17)$$

where $\tilde{f}_1$ result to be another free parameter and the other coefficients are completely determined by the four free parameters $(C_f, C_h, a, \tilde{f}_1)$. Similarly the functions $\tilde{h}_3(r)$ and $\tilde{f}_3(r)$ at order $O(e^{-3ar})$ can be found, obtaining two sixth degree polynomials in r but with no other free parameters appearing. The total number of free parameters of these solutions results then to be four, the correct number needed to connect these solutions with the $(1,0)^2_{r_0}$ family. Although we do not discuss the convergence of this expansion, we believe that a certain convergence radius r^* exists, such that for $r \gg r^*$, the solution is well approximated by (16). The numerical behavior found with our data is in agreement with this expansion already at first order, as we will show in Sec. III C.

III. NUMERICAL RESULTS AND THE STRUCTURE OF THE SPACETIME

A. Metric characterization with the shooting method

The shooting method has proven to be extremely useful for extracting the relevant physical properties of numerical solutions in quadratic gravity [7,26]. We consider the metric to be described by the weak field limit approximation (8) at large distances ($r = r_\infty$), and by the series expansion (10) at sixth order close to the throat ($r = r_T + r_\epsilon$). Equations (5) are then numerically integrated with guessed values of the parameters $(M, S_2^-, r_T, h_0, h_{1/2}, f_1)$ from both boundaries to a fitting radius $r = r_f$, where the continuity of $h(r)$, $f(r)$ and their derivatives is imposed with the use of a root finding algorithm. Once the convergence is achieved, this procedure fixes the value of the parameters $(r_T, h_0, h_{1/2}, f_1)$ that set the initial condition (13) at the other side of the throat for an additional integration toward $r \to +\infty$ (but with inverted sign for ρ), allowing us to study the second patch of the spacetime.

Throughout this analysis we integrated the equations using an adaptive stepsize method which switches between a midpoint and an implicit Euler methods, according to the stiffness of the system, with a tolerance of 10^{-14}, implemented using the WOLFRAM language. The continuity of the metric is obtained through the Newton's method used by the `FindRoot` function defined in this language, with a precision of 10^{-4}. The large distance radius has been fixed as $r_\infty = 15$ in order to have Yukawa corrections greater than the tolerance threshold, and the distance from the throat as $r_\epsilon = 10^{-3}$ in order to discard terms smaller than such threshold. The precise value of the fitting radius does not affect the accuracy of the shooting method, but is crucial for obtaining convergence efficiently; a value

sufficiently close to the throat, in particular we used $r_f = r_T + 5 \times 10^{-2}$, has been found optimal for our purposes. We specify here that the equations have been rescaled in terms of the Spin-2 particle mass m_2 in order to have dimensionless quantities, and then all the scales of the solutions will be determined by the only free parameter of the theory α; the length unit will be $l_2 = 4\sqrt{2\pi\alpha} l_p$, and the mass unit will be $m_2 = (4\sqrt{2\pi\alpha})^{-1} m_p$. For future reference, we remember that with the notation used in (8) the Schwarzschild mass parameter M has the dimension of length.

While for the one-parameter families described in [7,26] it was sufficient to fix either the event horizon or the stellar surface radii to find convergence for all the other parameters, the two degrees of freedom of no-sy WHs require some preliminary steps in our procedure. First of all, we have optimal convergence by fixing at the beginning of the integration the weak field parameters M and S_2^- instead of some throat parameter (e.g., the throat radius). We can mark the limits of the area in the M-S_2^- parameter space where no-sy WHs can be found with an exploratory scan of this space. At practical level this means that the equations of motion are integrated using (8) as initial conditions with values of M and S_2^- chosen on a grid, and the values for which the equations are singular at a finite radius $r > 0$ are saved in order to be used in the shooting method. As a cross check, the code where the shooting method is implemented never reaches convergence whenever initial values of M and S_2^- different from the one found with this scan are used. This preparatory integration is also used to find an educated guess for the parameters to use at the beginning of the shooting method, with a great increase in convergence efficiency. The preliminary scan of the parameter space is not only useful for improving convergence, but gave us relevant insight on the "phase diagram" of the theory, that is how the parameters M and S_2^- of the solutions determine the family they belong to. We will present the phase diagram of Einstein-Weyl gravity in further work.

B. The family of no-sy WH solutions

Before discussing the details of no-sy WH solutions, we would like to present the global trend for some of the parameters of the $(1,0)^2_{r_0}$ family. In particular we believe that the most informative parameters are the gravitational ones, M and S_2^-, the throat radius r_T, and the value of the temporal component of the metric at the throat h_0, that can be linked to the redshift of a photon emitted at such distance and measured at infinity by $z(r_T) = 1/\sqrt{h_0}$. In Fig. 1 we simultaneously show the area of the phase diagram populated by no-sy WHs, and the relations between the throat parameters r_T, h_0 and the gravitational ones M, S_2^-. No-sy WHs are found in two distinct regions: for a repulsive contribution of the Yukawa term in the potential (8), i.e. $S_2^- > 0$, the region of no-sy WHs is delimited by the Schwarzschild and non Schwarzschild black holes lines, and has a smooth transition into a region populated by horizonless solutions belonging to a logarithmic correction of the $(-1,-1)^1_0$ family; for an attractive contribution of the Yukawa term, i.e., $S_2^- < 0$, the region is still delimited by the Schwarzschild and non-Schwarzschild black holes lines, but is unbounded for large M and S_2^-. In both cases black holes appear as a transition between no-sy WHs and solutions of the $(-2,2)^1_0$ family. In particular we would like to stress the fact that, if we consider only positive mass solutions as physical, *no-sy WHs populate almost half of the physical region of the phase diagram*. If there are no criteria, e.g., symmetry arguments, for selecting solutions with $S_2^- = 0$, it is then natural to consider no-sy WHs as

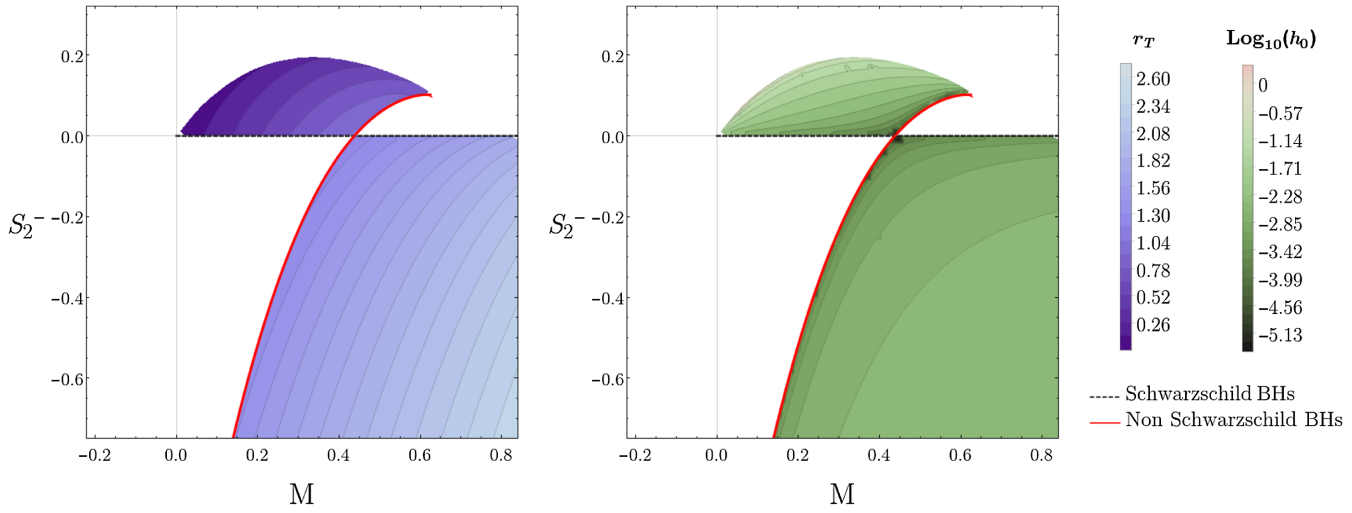

FIG. 1. Trend of the two main throat parameters in the phase diagram. In function of the gravitational parameters M and S_2^- we show the throat radius r_T in the left panel, and the redshift parameter h_0 in the right panel.

much more viable candidates than Schwarzschild black holes as generic vacuum solutions, even in the large mass limit.

The relations of the throat radius r_T and the redshift parameter h_0 are useful consistency checks. We see from Fig. 1 that the throat radius increases with an increasing mass, and in particular is consistent with the Schwarzschild mass-radius relation $r_H = 2M$ as the Yukawa charge goes to zero. We note that the throat radius increases also as the Yukawa charge decreases, and then in the large mass limit, where no-sy WHs are present only for negative values of S_2^-, no-sy WHs are always larger than the Schwarzschild black hole with the same mass. At last, as the gravitational parameters of a no-sy WH gets closer to the ones of a black hole, be it either of the Schwarzschild or non-Schwarzschild families, the redshift of a photon emitted at the throat increases, and the topological sphere defined by r_T becomes an infinite redshift surface in this limit. In other words, for large masses, if the Yukawa charge is sufficiently small no-sy WHs are optimal black hole mimickers.

C. The no-sy WH spacetime

We discuss here the main features of the no-sy WH solutions. The numerical results of the shooting method allowed us to characterize the no-sy WHs in the whole available space $\rho \in (-\infty, +\infty)$. We present the common behavior found for all the solutions studied, except for a small area located in the region of positive Yukawa charge. These exceptions correspond to solutions with the wormhole throat less than a maximum radius $r_T \leq \frac{1}{\sqrt{3}}$, in our unit, so we expect them to appear only at microscopical scales. For simplicity we do not discuss the behavior of these exceptions, instead we focus on all the other solutions, recalling that, on the contrary, they can have an arbitrary large radius. In what follows, we have chosen the region of spacetime with positive ρ as the asymptotically flat region. With this choice for $r \to +\infty$, $\rho \to +\infty$, the metric is determined by (8) with the line element

$$ds^2 = -\left(1 - \frac{2M}{r} + 2S_2^- \frac{e^{-m_2 r}}{r}\right) dt^2 + \frac{1}{1 - \frac{2M}{r} + S_2^- \frac{e^{-m_2 r}}{r}(1 + m_2 r)} dr^2 + r^2 d\Omega^2, \quad (18)$$

for $r \to r_T$, $\rho \to 0^{\pm}$, it is determined by (10), (13) with the line element

$$ds^2 = -h_0(1 \pm h_{1/2}(r - r_T)^{\frac{1}{2}} + O(r - r_T))dt^2 + \frac{1}{f_1(r - r_T) \pm O((r - r_T)^{\frac{3}{2}})} dr^2 + r^2 d\Omega^2, \quad (19)$$

and for $r \to +\infty$, $\rho \to -\infty$, it is determined by (16) with the line element

$$ds^2 = -C_h r^2 e^{-a r}(1 + O(e^{-a r}))dt^2 + C_f r^2 e^{-a r}(1 + O(e^{-a r}))dr^2 + r^2 d\Omega^2. \quad (20)$$

In Fig. 2 an example of no-sy WH spacetime is presented. In terms of the ρ-coordinate, the functions $h(\rho)$ and $f(\rho)$, as well as $g_{\rho\rho}(\rho)$ are smoothly matched from both the patches in $\rho = 0$.

The function $h(\rho)$ results to be monotonic, meaning that an observer would feel a gravitational force always in direction of decreasing ρ. This corresponds to an attractive central force in the asymptotically flat patch and a repulsive central force in the second patch.

In Fig. 3 we show the embedding diagram of no-sy WHs around $r = r_T$. This is built in order to have a radial displacement dr on the horizontal plane corresponding to a displacement of proper distance $d\tilde{r} = \frac{dr}{\sqrt{f(r)}}$ on the surface embedded. The embedding diagram is clearly similar to what we have for solutions with horizon, since in both cases $f(r)$ vanishes at a certain radius, however here the non symmetric behavior of such wormholes is explicit. Since $f(r)$ rapidly grows in the second patch, when $f(r) > 1$ the proper distance $d\tilde{r}$ becomes shorter than dr and the spacetime cannot be further embedded.

Finally we show the details of the metric for $\rho < 0$. In the previous plots the metric functions seem to have an exponential character in this region. We considered the ratio between the metric functions and their first derivatives. In particular in Fig. 4 we plotted the derivative of this ratio, which for an exact exponential is expected to vanish. We found the following limits

$$\frac{d}{dr}\left(\frac{f'(r)}{f(r)}\right) = \frac{f''(r)}{f(r)} - \left(\frac{f'(r)}{f(r)}\right)^2 \to \frac{2}{r^2}, \quad \frac{d}{dr}\left(\frac{h'(r)}{h(r)}\right) = \frac{h''(r)}{h(r)} - \left(\frac{h'(r)}{h(r)}\right)^2 \to -\frac{2}{r^2}, \quad (21)$$

that do not depend on the particular solution considered. This asymptotic behavior can be analytically integrated, finding again the first order of the asymptotically vanishing metric (16) and confirming that the solutions in the second patch are given by this expansion at large radius.

The nonflat behavior (16) brings several implications for the spacetime structure of the second patch.

With such behavior the asymptotic surface $r \to +\infty$, $\rho \to -\infty$ results located at a finite proper distance from the wormhole throat. Indeed the proper radial distance is given by

$$\tilde{r}_{\max} = \int_{r_T}^{\infty} \frac{dr}{\sqrt{f(r)}}, \quad (22)$$

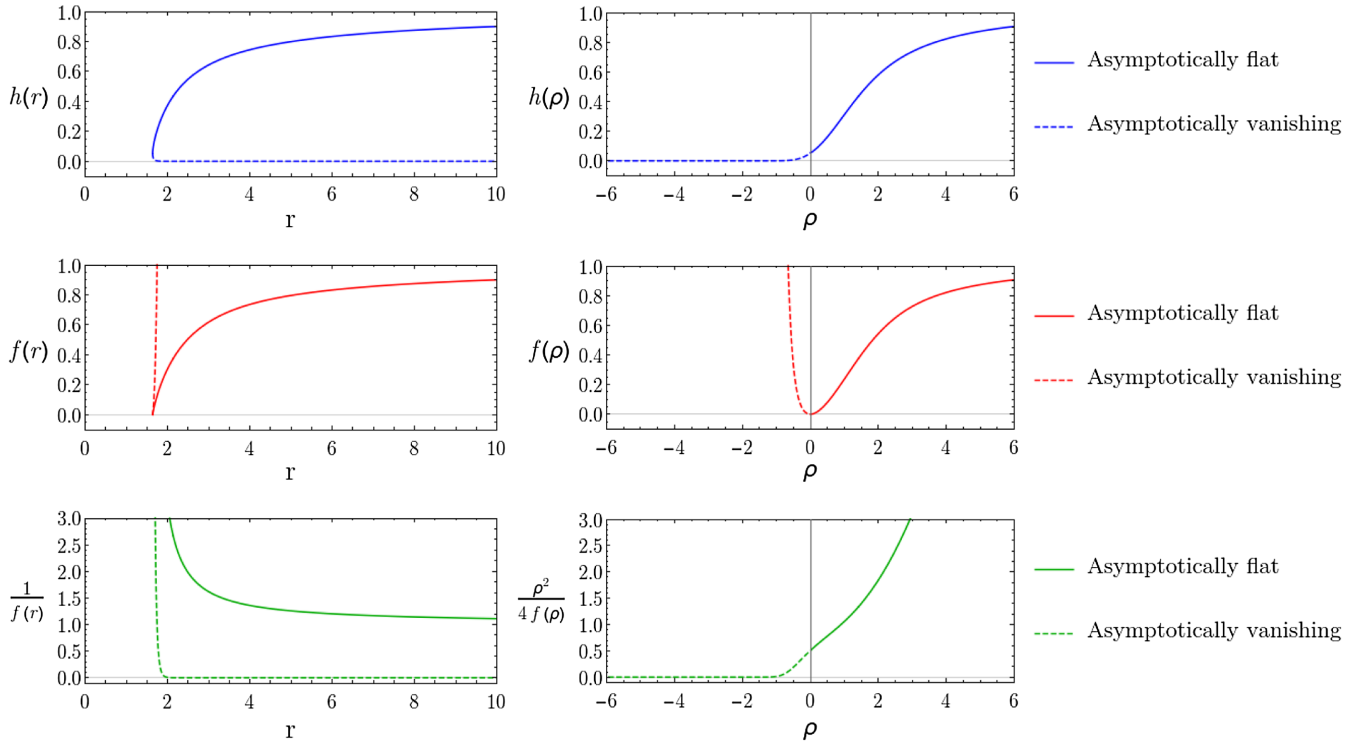

FIG. 2. Metric of a no-sy WH solution with $M = 0.5$ and $S_2^- = -0.3$: in the panels on the left the metric is in function of the r-coordinate, while in the panels on the right is in function of the ρ-coordinate; solid and dashed lines indicate whether we are in the asymptotically flat or in the asymptotically vanishing patch, respectively.

and this integral converges with $f(r)$ interpolated between (10) and (16). The proper volume of the entire $\rho < 0$ region is finite: it is given by

$$V_p = 4\pi \int_{r_T}^{\infty} dr \frac{r^2}{\sqrt{f(r)}}, \tag{23}$$

that converges again.

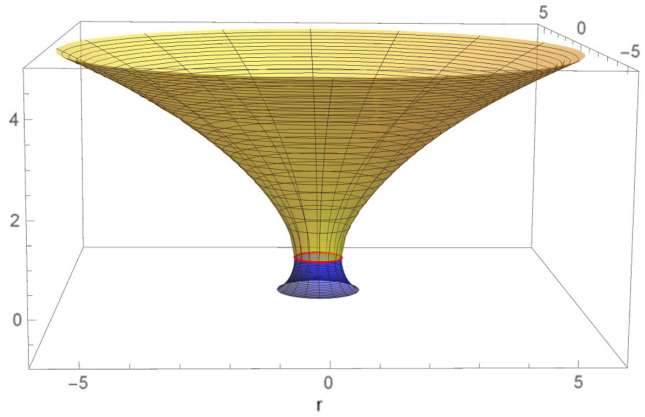

FIG. 3. Embedding diagram of a no-sy WH solution with $M = 0.55$ and $S_2^- = 0.14$: the yellow part corresponds to the $\rho > 0$ region, the red curve corresponds to $r = r_T$, the blue part corresponds to the $\rho < 0$ region.

From the monotonicity of $h(\rho)$, the surface $r \to +\infty$ also results to be attractive.

These considerations completely changes the nature of the second patch and highlights the nonsymmetric nature of these solutions. In Sec. IV we focus on the peculiar features of the metric at the surface $r \to +\infty$ of the second patch.

1. Geodesic dynamics and photon sphere

Before we discuss the details of the asymptotic surface of the second patch, we show the geodesic dynamics of the no-sy WH spacetime. We start recalling that a general geodesic in a static spherically symmetric spacetime can be defined as the integral line of the vector field V^μ with components

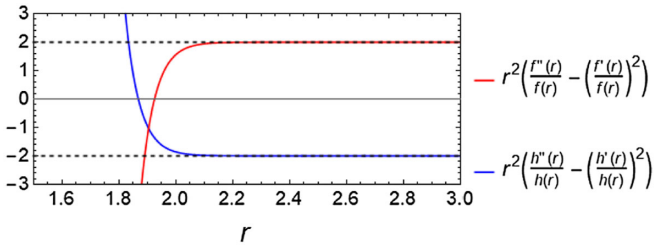

FIG. 4. Details of the metric in the asymptotically vanishing region of a no-sy WH solution with $M = 0.5$ and $S_2^- = -0.3$.

$$V^t = \frac{dt}{d\tau} = \frac{E}{h(r)},$$
$$V^r = \frac{dr}{d\tau} = \pm\sqrt{f(r)\left(\frac{E^2}{h(r)} - \frac{L^2}{r^2} + \kappa\right)},$$
$$V^\theta = \frac{d\theta}{d\tau} = 0,$$
$$V^\phi = \frac{d\phi}{d\tau} = \frac{L}{r^2}, \tag{24}$$

with $\kappa = -1$ and τ the proper-time for a timelike geodesic, or $\kappa = 0$ and τ an affine parameter for a null geodesic, and where we considered $\theta = \pi/2$ without loss of generality.

First we note that the wormhole nature is manifest in the geodesic dynamics around the throat. Indeed, recalling the transformation (11), the radial component in (24) can be written in terms of ρ as

$$\frac{d\rho}{d\tau} = \pm\sqrt{\frac{f(r)}{(r-r_T)}\left(\frac{E^2}{h(r)} - \frac{L^2}{r^2} + \kappa\right)}. \tag{25}$$

With $f(r)$ given by the metric around the throat (10), Eq. (25) can be integrated obtaining a smooth geodesic that goes from positive to negative ρ. Together with this, Eq. (24) tells that $\frac{dr}{d\tau}$ is forced to vanish at the throat. On the contrary, with this type of metric it is not possible to build a differentiable geodesic that goes from $r > r_T$ to $r < r_T$, confirming the interpretation of the $(1,0)^2_{r_0}$ as a wormhole solution family.

The second thing we want to highlight is that, if a free-falling object enters into the wormhole throat from the asymptotically flat patch it will proceed until it reaches the surface $r \to +\infty$ of the second patch.

In order to enter into the wormhole, the radical argument in (25) must be positive: around the throat we have $f(r) = f_1(r-r_T) + O((r-r_T)^{\frac{3}{2}})$ so for positive f_1 we get the condition

$$\frac{E^2}{h(r_T)} > \frac{L^2}{r_T^2} - \kappa. \tag{26}$$

Once entered in the second patch, $\frac{d\rho}{d\tau}$ cannot vanish, indeed we have

$$\frac{E^2}{h(r)} > \frac{E^2}{h(r_T)} > \frac{L^2}{r_T^2} - \kappa > \frac{L^2}{r^2} - \kappa, \tag{27}$$

since $h(r)$ results decreasing in the asymptotically vanishing region. This means that a free-falling object will inevitably reach $\rho = -\infty$, since it is attracted by the gravitational force, and the angular momentum conservation contributes in the same direction.

Moreover this happens in a finite interval of proper time. The proper time interval needed to fall into this surface is

$$\tau_s = \int_{r(0)}^{\infty} \frac{1}{\sqrt{f(r)(\frac{E^2}{h(r)} - \frac{L^2}{r^2} + \kappa)}} dr, \tag{28}$$

that is certainly convergent due to the asymptotic behavior $\frac{f(r)}{h(r)} = O(\frac{e^{2ar}}{r^4})$.

For a distant observer in the asymptotically flat patch instead, a particle falls into the wormhole throat in a finite time interval, but the time needed to reach the surface $\rho \to -\infty$ results divergent, as it is given by

$$t = \int_{r(0)}^{r(t)} \frac{E}{\sqrt{f(r)(E^2 h(r) - (\frac{L^2}{r^2} + \kappa)h(r)^2)}} dr. \tag{29}$$

Around the throat we have $h(r) = h_0 + O(r - r_T)$ and $f(r) = f_1(r-r_T) + O((r-r_T)^{\frac{3}{2}})$ so the integral in (29) converges to a finite time interval for the distant observer.

On the other hand, with the asymptotic behavior (16) the integrand in (29) tends to a constant but it must be integrated to infinity, so the integral diverges for $r(t) \to +\infty$.

The geodesic behavior around the throat implies that the photon sphere (see e.g., [27]) of no-sy WHs is always located in the asymptotically flat patch. For a distant observer in this patch, a no-sy WH appears like an ultracompact object located inside its photon sphere. The asymptotic surface $\rho \to -\infty$ appears like an attractive horizon "inside" the throat. Instead any free-falling observer in the second patch falls into this surface in a finite amount of proper time but it can always spend energy to escape.

IV. THE NATURE OF THE SINGULARITY AND DISCUSSION

The peculiar properties of the spacetime at the hypersurface defined by $r \to +\infty$ in the asymptotically vanishing patch strongly suggest that it should be a singular region. Indeed the behavior (16) implies the following limits for the curvature invariants:

$$R = 0 \quad \text{for } r \to +\infty,$$
$$R_{\mu\nu}R^{\mu\nu} = O\left(\frac{e^{2ar}}{r^6}\right) \quad \text{for } r \to +\infty,$$
$$R_{\mu\nu\rho\sigma}R^{\mu\nu\rho\sigma} = O\left(\frac{e^{2ar}}{r^6}\right) \quad \text{for } r \to +\infty; \tag{30}$$

with the Ricci scalar being identically zero for our e.o.m., but with divergent squared Ricci tensor and Kretschmann scalar. Quite interestingly, the squared Weyl tensor results regular due to a cancellation between the divergent part of the Kretschmann scalar and the squared Ricci tensor.

In particular using the precise result for $\tilde{h}_3(r)$ and $\tilde{f}_3(r)$ in (16) it is possible to prove the limit

$$C_{\mu\nu\rho\sigma}C^{\mu\nu\rho\sigma} = 3m_2^4 \quad \text{for } r \to +\infty, \tag{31}$$

that does not depend on the particular solution considered. This result is crucial for the application of the finite action principle [28], that is getting much attention in recent times for its applications in quadratic theories of gravity [29–31]. We also note that, beside the singular nature of the curvature invariants, the fact that a timelike geodesic reaches an infinite radius in a finite proper time is a strong indication that the spacetime is geodesically incomplete. As it is clear that the hypersurface at $r \to +\infty$ is a singular region, it is a new kind of singularity with unique physical properties. To begin with, the causal structure of the spacetime is radically different from the standard solutions of general relativity. As shown in the conformal diagram of figure 5, we see that the causal structure of a no-sy WH is equivalent to the one of a maximally extended Minkowski with a singularity at the "internal" $\mathcal{J}_I^+$ and $\mathcal{J}_I^-$. This is not surprising, considering that the t-r sector of a no-sy WH spacetime is conformally equivalent to the Minkowski one after the coordinate transformation

$$ds^2 = h(r)(-dt^2 + dr^{*2}) + r^2 d\Omega^2, \tag{32}$$

where the tortoise coordinate goes to zero at the throat. The relevant information that is manifestly shown in Fig. 5, however, is that the singularity is at the edges of the causal structure. In other words, a distant observer can communicate

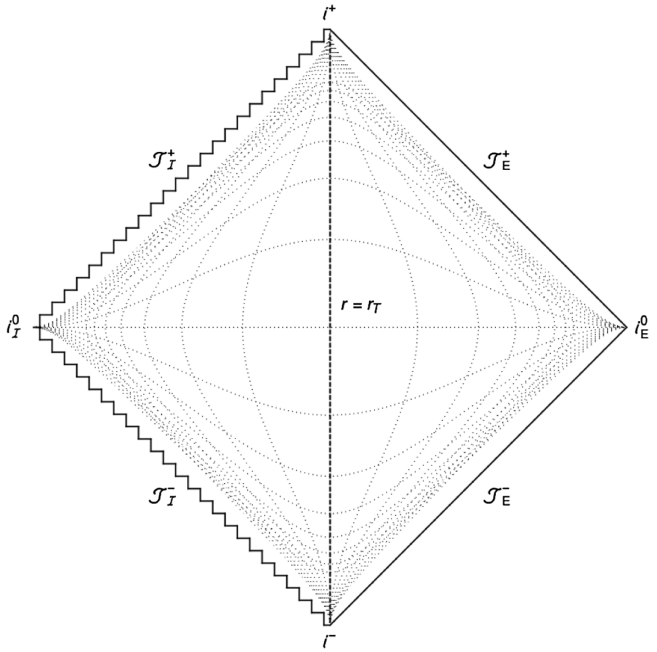

FIG. 5. Conformal diagram of a no-sy WH spacetime; the dotted lines indicate surfaces of constant time and radius.

with the singularity only in an infinite amount of time. Furthermore, if we recall the definition of the redshift of a photon emitted at radius r and measured at infinity $z(r) = \frac{1}{\sqrt{h(r)}}$, we see that the singularity is actually on an infinite redshift surface and, as for an event horizon, an infinite amount of energy is required to leave it. The singularity is therefore naked only in its infinite past section, and can be interpreted as the equivalent of a white hole singularity. The problem of dealing with naked singularities in no-sy WH spacetimes is then reduced to finding a collapse mechanism for the generation of such objects; however, we postpone this study to further work.

We now consider the behavior of a congruence of infalling geodesics with tangent vector (24), where with infalling we mean that has a negative V^r in the asymptotically flat patch, and a positive V^r in the asymptotically vanishing one. Following the discussion in chapter 4 of [32], we consider the vector field Z^μ, which represent the separation of points in nearby geodesics, that satisfies the equation

$$\frac{\mathrm{d}}{\mathrm{d}\tau} Z^\mu = B^\mu{}_\nu Z^\nu, \tag{33}$$

where we have defined the deviation tensor

$$B_{\mu\nu} = h^\rho{}_\mu h^\sigma{}_\nu \nabla_\rho V_\sigma \tag{34}$$

with $h_{\mu\nu}$ being the metric of either the hypersurface orthogonal to the geodesic in the timelike case or the surface transverse to the geodesic in the null case. The first thing we want to highlight is that the expansion scalar

$$\theta = h^{\mu\nu} B_{\mu\nu} \tag{35}$$

does not go to a *negative* infinite value at the singularity, as it happens in the Schwarzschild case, but it goes to a *positive* infinite value as in the limit of outgoing geodesics reaching spatial infinity in asymptotically flat solutions. However, the peculiar feature here is that *the expansion scalar goes to infinity in a finite proper time*. It is in fact possible to prove that the expansion scalar at large radii satisfies

$$\theta(\tau) > \frac{1}{(\tau_s - \tau)^\alpha}, \tag{36}$$

with $0 < \alpha < 1$ and τ_s being the proper time (or the affine parameter) at which the geodesic reaches the singularity, and then that it diverges in the limit $\tau \to \tau_s$. The second thing we want to highlight is the behavior of the deviation vector Z^μ. If we restrict ourselves to radial geodesics, using the definition of proper time (28) and the asymptotic expansion (15) we can solve the differential equations (33) close to the singular surface as

$$Z^\mu = \begin{cases} Z^t(r) \sim c^t r, \\ Z^r(r) \sim c^r r, \\ Z^\theta(r) \sim c^\theta r, \\ Z^\phi(r) \sim c^\phi r, \end{cases} \qquad Z^\mu = \begin{cases} Z^t(r) \sim c^t, \\ Z^r(r) \sim c^r, \\ Z^\theta(r) \sim c^\theta r, \\ Z^\phi(r) \sim c^\phi r, \end{cases} \tag{37}$$

in the timelike and null cases respectively. While null geodesics diverge only for geometrical aspects, timelike geodesics experience extreme tidal forces in the radial and temporal directions, that actually diverge as they get closer to the singularity. The presence of such disruption of timelike observers at a finite value of the proper time has a remarkable resemblance with the big rip cosmological scenario, where the expansion of the universe diverges in a finite amount of cosmological time. This big riplike singularity is however localized inside a topological sphere of radius $r = r_T$ for an observer in the asymptotically flat patch, and has an "origin" in the topological sphere of radius $r = r_T$ for an observer in the asymptotically vanishing one.

With the information at our disposal, we can now have an insight on how no-sy WHs are perceived by observers:

(i) *infalling* observers coming from the asymptotic flat patch are attracted by the no-sy WH just as by other compact objects, but after they have reached the radius $r = r_T$ they start to feel a repulsive force, and tidal forces in all directions: they are quickly pushed away to spatial infinity, and the tidal forces become so strong that are able to break all the binding energies and completely disrupt the observer in a finite amount of proper time, just like in the big rip cosmological scenario; however, in principle observers can always turn on a rocket and escape their fate;

(ii) *distant* observers in the asymptotically flat patch see an attractive object enclosed inside the topological sphere of radius $r = r_T$; the object is smaller than its photon sphere, and the light emitted outside this sphere will be absorbed by the object; however, particles can emit light from inside the object, but this emission is expected at extremely low frequencies: first of all photons are exponentially redshifted, and the temperature of a ball of gas is expected to decrease, as the volume increases as can be seen from (37); moreover, distant observers will never see the disruption of the infalling gas, that is instead perceived as "frozen" inside the object.

In conclusion, we can interpret no-sy WHs as black hole mimickers with a "singularity by disruption" instead of a "singularity by compression" that, for this reason, is always avoidable.

V. CONCLUSIONS

In this paper we give a complete description of the nonsymmetric wormhole (no-sy WH) type of solutions of Einstein-Weyl gravity. With different analytical approximations, and using a shooting method procedure, we managed to link the properties of the spacetime at large distances to the ones close to the wormhole throat, and also to explore the second patch of the spacetime. No-sy WH solutions are characterized by an asymptotically flat patch, where they are described by a newtonian potential with a Yukawa correction, and by an asymptotically vanishing patch, where geodesics reach a singular surface in a finite proper time; the two patches are joined at the "throat," that is the topological sphere with the minimum radius that can be reached in this kind of spacetime. The values of the ADM mass and the Yukawa charge for which we have this type of solutions reveal that no-sy WHs populate a large area of the physical part of the parameter space of the theory, and that they are a much more viable candidate to be the generic vacuum solution of Einstein-Weyl gravity than black holes. The behavior of the metric close to the throat, instead, suggests that no-sy WHs are optimal black hole mimickers, with the throat being an extremely high redshift surface, and with the photon sphere having a radius always larger than the throat. The singularity in the asymptotically vanishing patch has the peculiar behavior of resembling the big rip cosmological singularity, with the presence of extreme tidal forces in all directions that completely disrupt timelike observers in a finite proper time. Despite having no horizons, the singularity results naked only in the infinite past, being at the edges of the causal structure of the solution. The absence of horizons, however, guarantees that there are no trapped surfaces, and with enough energy an outgoing geodesics can always escape from the singularity and reach the asymptotically flat region. All these properties suggest that no-sy WHs might be the substitutes predicted by quadratic gravity to black hole solutions. In order to make a definite statement, however, is fundamental to address the stability of the solutions, that we plan to tackle in future, and subsequently the formation of no-sy WHs, their rotating counterparts, and the properties of an accretion disk surrounding them.

ACKNOWLEDGMENTS

S. S. would like to thank Massimiliano Rinaldi for his useful advice and stimulating discussions. This work has been supported by the INFN grant FLAG and the TIFPA—Trento Institute for Fundamental Physics and Applications. A. Z. would like to thank Damiano Anselmi for the support. We would like to thank Frank Saueressig for the important comments on the manuscript.

[1] H. Lu, A. Perkins, C. Pope, and K. Stelle, Phys. Rev. Lett. **114**, 171601 (2015).
[2] J. Podolsky, R. Švarc, V. Pravda, and A. Pravdova, Phys. Rev. D **98**, 021502 (2018).
[3] J. Podolsk, R. Švarc, V. Pravda, and A. Pravdova, Phys. Rev. D **101**, 024027 (2020).
[4] F. Saueressig, M. Galis, J. Daas, and A. Khosravi, Int. J. Mod. Phys. D **30**, 2142015 (2021).
[5] H. L, A. Perkins, C. Pope, and K. Stelle, Phys. Rev. D **92**, 124019 (2015).
[6] K. Goldstein and J. J. Mashiyane, Phys. Rev. D **97**, 024015 (2018).
[7] A. Bonanno and S. Silveravalle, Phys. Rev. D **99**, 101501 (2019).
[8] S. Capozziello and M. de Laurentis, Phys. Rep. **509**, 167 (2011).
[9] G. J. Olmo, D. Rubiera-Garcia, and A. Wojnar, Phys. Rep. **876**, 1 (2020).
[10] S. Capozziello, M. De Laurentis, R. Farinelli, and S. D. Odintsov, Phys. Rev. D **93**, 023501 (2016).
[11] A. V. Astashenok, S. Capozziello, and S. D. Odintsov, J. Cosmol. Astropart. Phys. 12 (**2013**) 040.
[12] K. Stelle, Phys. Rev. D **16**, 953 (1977).
[13] D. Benedetti, P. F. Machado, and F. Saueressig, Nucl. Phys. **B824**, 168 (2010).
[14] D. Benedetti, P. F. Machado, and F. Saueressig, Mod. Phys. Lett. A **24**, 2233 (2009).
[15] Y. Hamada and M. Yamada, J. High Energy Phys. 08 (2017) 070.
[16] R. Percacci, *An Introduction to Covariant Quantum Gravity and Asymptotic Safety*, 100 Years of General Relativity Vol. 3 (World Scientific, Singapore, 2017).
[17] M. Reuter and F. Saueressig, *Quantum Gravity and the Functional Renormalization Group: The Road towards Asymptotic Safety* (Cambridge University Press, Cambridge, England, 2019).
[18] D. Anselmi, J. High Energy Phys. 06 (2017) 086.
[19] D. Anselmi and M. Piva, J. High Energy Phys. 05 (2018) 027.
[20] R. R. Caldwell, Phys. Lett. B **545**, 23 (2002).
[21] J. Arrechea, C. Barceló, R. Carballo-Rubio, and L. J. Garay, Phys. Rev. D **101**, 064059 (2020).
[22] J. Oliva, D. Tempo, and R. Troncoso, Int. J. Mod. Phys. A **24**, 1528 (2009).
[23] S. Silveravalle, Nuovo Cimento Soc. Ital. Fis. C (to be published).
[24] K. S. Stelle, Gen. Relativ. Gravit. **9**, 353 (1978).
[25] A. Perkins, Static spherically symmetric solutions in higher derivative gravity, Ph.D. thesis, Imperial College, 2016.
[26] A. Bonanno and S. Silveravalle, J. Cosmol. Astropart. Phys. 08 (2021) 050.
[27] C.-M. Claudel, K. S. Virbhadra, and G. F. R. Ellis, J. Math. Phys. (N.Y.) **42**, 818 (2001).
[28] J. D. Barrow and F. J. Tipler, Nature (London) **331**, 31 (1988).
[29] J.-L. Lehners and K. S. Stelle, Phys. Rev. D **100**, 083540 (2019).
[30] J. N. Borissova and A. Eichhorn, Universe **7**, 48 (2021).
[31] J. Chojnacki and J. Kwapisz, Phys. Rev. D **104**, 103504 (2021).
[32] S. W. Hawking and G. F. R. Ellis, *The Large Scale Structure of Space-Time*, Cambridge Monographs on Mathematical Physics (Cambridge University Press, Cambridge, England, 2011).